



Cite this: *Polym. Chem.*, 2022, **13**, 5700

## Water-soluble copolymers and their hydrogels with pH-tunable diverse thermoresponsive behaviors enabled by hydrogen bonding†

Ruidong Cheng,<sup>a,b</sup> Jie Jiang,<sup>a</sup> Junbo Hou,<sup>a</sup> Guo Li,<sup>ID</sup><sup>b</sup> Jinqiang Jiang,<sup>ID</sup><sup>\*b</sup> and Yue Zhao<sup>ID</sup><sup>\*a</sup>

Water-soluble copolymers of poly(acrylic acid-*co*-*N*-vinylcaprolactam) (PAN) and poly(acrylic acid-*co*-*N*-vinylcaprolactam-*co*-dimethyl acrylamide) (PAND) were synthesized and found to exhibit opposite, and pH-tunable, UCST (upper critical solution temperature) and LCST (lower critical solution temperature) thermosensitive solubility in aqueous solution, respectively. For PAN (UCST), the insoluble state is determined by hydrogen bonding between comonomer units (AA–NVCL and AA–AA), and the solubility is obtained on heating as these intra- and inter-polymer H-bonds are weakened, promoting the solubilization of polymer chains by water molecules. For PAND (LCST), the hydrogen bonding between comonomer units still plays the determining role, for which the hydrophobic H-bonded “complex” of AA–NVCL and AA–AA exerts a similar effect as a hydrophobic comonomer on the LCST of poly(dimethyl acrylamide) (PDMA), causing the hydration–dehydration transition upon heating of DMA segments in PAND. UCST and LCST hydrogels were prepared using PAN and PAND, respectively, and used to demonstrate pH sensitivity-enabled information recording and opposite encryption/decryption processes through temperature change.

Received 11th August 2022,  
Accepted 14th September 2022

DOI: 10.1039/d2py01044e

rsc.li/polymers

## Introduction

Thermoresponsive polymers (TRPs) in solution can undergo a reversibly soluble-insoluble volume transition depending on the environmental temperature.<sup>1–3</sup> Basically, they are soluble at temperatures below the lower critical solution temperature (LCST)<sup>4–6</sup> or above the upper critical solution temperature (UCST),<sup>7–9</sup> but become insoluble above the LCST or below the UCST. This characteristic property enables smart polymer manipulation *via* “on–off” switchable control with temperature. Therefore, they are used in a wide array of applications, including optical devices,<sup>10,11</sup> drug delivery,<sup>12–14</sup> coatings,<sup>15,16</sup> catalysts,<sup>17–19</sup> sensors,<sup>20–22</sup> and actuators.<sup>23–25</sup> Currently, endowing TRPs with tunable LCST or UCST generated from common and cost-effective monomers is becoming an essential consideration in both practical and academic research.

Both LCST and UCST water-soluble polymers exhibit a balance between polymer–polymer interactions and polymer–water interactions, which is critical for the molecular designing of thermoresponsive polymers.<sup>2,26–28</sup> Generally, temperature variations influence the entropy of solvation of the polymer chains in an aqueous solution, leading to the LCST behavior with polymers undergoing transition from a hydrophilic coil to a hydrophobic globule state.<sup>29</sup> It is common practice to copolymerize hydrophilic or hydrophobic monomers to tune the LCST of polymers.<sup>30</sup> For example, poly(*N,N*'-dimethyl acrylamide) (PDMA) is water soluble, but its LCST, expected to be higher than 100 °C, can be decreased to an observable range (0–100 °C) through copolymerization with hydrophobic styrene.<sup>31</sup> The behavior of UCST, on the other hand, is governed by enthalpy.<sup>32–34</sup> Strong polymer–polymer interactions, such as electrostatic interactions<sup>35–37</sup> and hydrophobic association,<sup>9,38,39</sup> become increasingly prominent on cooling, resulting in phase separation. At temperatures between 0 and 100 °C, only a few polymers are known to display the UCST behavior.<sup>34</sup> The most commonly reported polymers with the UCST behavior in water are zwitterionic polymers and the zwitterionic nature makes the UCST sensitive to a salt or electrolyte.<sup>35–37</sup> Recent work has shown that water-soluble poly(acrylic acid) (PAA) can be copolymerized with acrylonitrile to yield a thermoresponsive polymer exhibiting the UCST behavior, which is driven by the combined effect of hydrogen

<sup>a</sup>Département de Chimie, Université de Sherbrooke, Sherbrooke, Quebec J1K 2R1, Canada. E-mail: yue.zhao@usherbrooke.ca

<sup>b</sup>Key Laboratory of Syngas Conversion of Shaanxi Province, Key Laboratory of Applied Surface and Colloid Chemistry, Ministry of Education, School of Chemistry and Chemical Engineering, Shaanxi Normal University, Xi'an, Shaanxi Province, 710062, China. E-mail: jiangjq@snnu.edu.cn

† Electronic supplementary information (ESI) available: Supplementary Fig. S1–S14. Polymer synthesis and characterization; preparation of polymer hydrogels; additional control experiments. See DOI: <https://doi.org/10.1039/d2py01044e>

bonding between the carboxylic acid groups and hydrophobic interaction among the acrylonitrile moieties.<sup>40</sup> Additionally, when copolymerized with a hydrophobic comonomer such as acrylonitrile,<sup>38,39</sup> styrene,<sup>41</sup> or azobenzene,<sup>9</sup> the water-soluble polymer of poly(acrylamide) (PAM) can also display the UCST. All these previous findings indicate that more water-soluble PAA or PAM based copolymers may be synthesized which can exhibit the UCST behavior in an aqueous environment. More interestingly, in the same vein, if the hydrophobic character of a comonomer or comonomers can be adjusted by a stimulus, the stimulus can be utilized to tune the UCST and/or LCST behaviors of such copolymers. It is thus of continuing interest to develop approaches for TRPs with stimulus-controllable UCST or LCST and explore their potential applications. Herein, we show pH-tunable UCST and LCST from random copolymers comprising all water-soluble monomers, resulting from hydrogen-bonded comonomers acting as a hydrophobic domain in the polymers.

In the present study, we performed free radical polymerization to incorporate the hydrophilic comonomer *N*-vinylcaprolactam (NVCL) into PAA to bring the UCST to an ambient temperature range at various pH levels. Due to the active protons (COOH) and electro-negative carbonyl groups (C=O from NVCL) in P(AA-*co*-NVCL) (PAN) at pH < 3.0, their hydrogen bonding is highly stable.<sup>42</sup> In contrast, the hydrogen bonding of AA-AA dimers is relatively weak and can be dissociated by heating.<sup>40</sup> Therefore, the strength of hydrogen

bonding in the copolymer and its UCST as revealed from the solution cloud point can be tuned by adjusting the monomer ratio and pH of the solution. Interestingly, when a third hydrophilic comonomer, dimethyl acrylamide (DMA), was introduced, the thermoresponsiveness of the copolymer of P(AA-*co*-NVCL-*co*-DMA) (PAND) could be converted into the LCST-type over the same pH range. Moreover, pH-tunable thermo-responsive hydrogels of PAN and PAND have been prepared and used for demonstrating information recording and encryption/decryption applications.

## Results and discussion

### Copolymer synthesis

A series of PAN and PAND random copolymers with different monomer molar ratios were synthesized *via* free radical polymerization. The synthetic schemes and the acronyms of the monomers and copolymers are shown in Fig. 1. The main characteristics of the synthesized copolymers, including the copolymer composition with respect to the feed ratio of monomers as well as their average molecular weights and dispersities, are presented in Table 1. The results of <sup>1</sup>H NMR analysis reveal that the NVCL content of the PAN polymer is always less than in the feed, likely because NVCL has a lower reactivity than acrylic acid.<sup>43</sup> In contrast, the contents of AA, NVCL and DMA in the copolymers of PAND are comparable to or slightly different from those in the feed (Table 1). It should be emphasized that as long as the low molar mass region is not reached, the broadness of the molar mass distribution (expressed by  $M_w/M_n$ ) has little effect on the cloud point.<sup>34</sup> For PAN samples, the subscript in the acronym indicates the mol% of NVCL units, while for PAND samples, it is the mol% of DMA units. Details about the syntheses are given in the ESI.† Of the copolymers synthesized, except for PAN<sub>11.6%</sub> that is insoluble in deionized water primarily due to the dense hydrogen bonds formed between AA and NVCL comonomer units,<sup>42</sup> all are highly soluble in deionized water. PAN<sub>5.3%</sub> and PAND<sub>52.6%</sub> were chosen to study the thermoresponsive behaviors through cloud point measurement of their aqueous solutions. At a

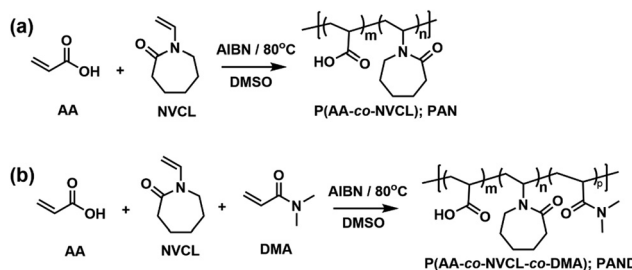


Fig. 1 The free radical polymerization of (a) P(AA-*co*-NVCL) (denoted as PAN) and (b) P(AA-*co*-NVCL-*co*-DMA) (PAND).

Table 1 Characteristics of the synthesized copolymers: P(AA-*co*-NVCL) (PAN) and P(AA-*co*-NVCL-*co*-DMA) (PAND)

Sample number	Monomer ratio (mol/mol%)			Yield (%)	$M_n^c$ (kg mol <sup>-1</sup> )	$M_w/M_n^c$
	AA	NVCL	DMA			
PAN <sub>3.7%</sub>	95.0 <sup>a</sup> (96.3) <sup>b</sup>	5.0 (3.7)	—	93.6	33.7	3.4
PAN <sub>4.4%</sub>	92.5 (95.6)	7.5 (4.4)	—	87.7	27.7	3.1
PAN <sub>5.3%</sub>	90.0 (94.7)	10.0 (5.3)	—	67.8	30.1	3.3
PAN <sub>11.6%</sub>	85.0 (88.4)	15.0 (11.6)	—	70.9	—	—
PAND <sub>52.6%</sub>	45.0 (40.2)	5.0 (7.2)	50.0 (52.6)	72.5	34.3	3.7
PAND <sub>58.1%</sub>	40.5 (37.1)	4.5 (4.8)	55.0 (58.1)	69.2	34.0	4.4
PAND <sub>64.5%</sub>	36.0 (30.1)	4.0 (5.4)	60.0 (64.5)	70.8	41.9	3.8
PAND <sub>68.5%</sub>	32.0 (26.5)	3.6 (5.0)	64.4 (68.5)	73.3	40.8	4.2

<sup>a</sup> Monomer ratio in the feed. <sup>b</sup> Monomer ratios in the product, estimated from <sup>1</sup>H NMR in d<sub>6</sub>-DMSO. <sup>c</sup> Number-average ( $M_n$ ) and weight-average ( $M_w$ ) molar masses determined by size exclusion chromatography (SEC) with deionized water as the eluent.

copolymer concentration of 5.0 mg mL<sup>-1</sup>, the solutions of PAN<sub>5.3%</sub> and PAND<sub>52.6%</sub> have a pH of 3.0 and 3.5, respectively.

### UCST behaviour of PAN

The PAN samples exhibit a water solubility transition in response to a pH change. This can be noticed visually from the pictures of the solutions in Fig. 2a. While the solution remains transparent at pH 3.0, it turns turbid at pH 2.0, indicating that the water solubility switching of PAN<sub>5.3%</sub> occurs over the pH change. Meanwhile, the copolymer solution exhibits the UCST behavior, being insoluble at lower temperatures (25 °C) but soluble when heated above a certain critical temperature (50 °C). The pH-dependent UCST shift is further revealed by monitoring the change in the cloud point of their aqueous solution. All measurements were conducted in deionized water at a polymer concentration of 5.0 mg mL<sup>-1</sup> and a heating rate of 1.0 °C min<sup>-1</sup>. As shown in Fig. 2b, the transmittance vs. temperature curve for the solution of PAN<sub>5.3%</sub> (pH 3.0) is nearly constant, indicating that there is no observable thermoresponsive solubility change. However, when HCl was gradually added to lower its pH, the polymer solution exhibited the phase separation in the measured temperature range, showing significant turbidity at low temperatures and high transmittance at elevated temperatures (UCST-type). The cloud point of PAN<sub>5.3%</sub> solution increases from 13.8 to 39.0 °C with decreasing pH from 2.5 to 1.3 (Fig. S9b†). Given the presence of AA in the copolymer structure, a decrease in the pH indicates more protonated COOH groups and reduced water solubility.<sup>40</sup> On the other hand, the hydrogen bonds between AA-

AA and AA–NVCL are enhanced with the protonation of the COOH groups at pH < pK<sub>a</sub>.<sup>42</sup> The PAN samples exhibit a clear cloud point increase in response to pH decrease, which implies that H-bonds between monomer units, especially the stronger H-bonds between AA and NVCL, impart hydrophobic character to the copolymer, and that this resulting H-bonding hydrophobicity is easily tunable through pH change. Furthermore, the thermoresponsiveness of the copolymer shows a typical concentration dependence of the phase transition temperature for polymeric solutes.<sup>2,40</sup> At pH 2.0, the cloud point of PAN<sub>5.3%</sub> increases from 13.0 to 39.0 °C when the concentration of the copolymer increases from 1.0 to 5.0 mg mL<sup>-1</sup> (Fig. S10a†). These results are consistent with other hydrogen bonding based UCST polymers.<sup>40</sup> On the other hand, the effect of the copolymer composition (AA/NVCL ratio) on the cloud point was investigated. As shown in Fig. 2c, the cloud point changes from 19.2 to 39.0 °C when the NVCL content rises from 3.7 to 5.3 mol%. The copolymers with a higher NVCL content exhibit a higher cloud point, owing to the stronger hydrophobic interactions from H-bonded AA–NVCL complexes.<sup>42</sup> Fig. 2d shows the highly reversible on-off thermo-switching of the solubility of PAN<sub>5.3%</sub> in aqueous solution (5.0 mg mL<sup>-1</sup>, pH 2.0) under nine repeated heating and cooling cycles. As can be seen, the transparency of the copolymer solution quickly increases from 1.5% to 98.0% upon heating to 50 °C and decreases to its original low transparency value upon subsequent cooling to 25 °C within 5 min.

### LCST behaviour of PAND

By synthesizing PAND, we wanted to know how the presence of a third water-soluble monomer, DMA, in the copolymer structure can impact the thermoresponsive behaviors. Even though DMA can in principle form H-bonds with AA to compete with H-bonds between NVCL and AA, it was found that PAND with lower DMA contents still displayed UCST-type thermosensitivity like PAN. This is likely due to the fact that NVCL-AA H-bonding is much stronger than DMA-AA H-bonding owing to the greater electronegativity of the carbonyl group in NVCL.<sup>42,44</sup> In other words, the H-bonded AA–NVCL hydrophobic domain predominates and thus the UCST behavior is retained. Interestingly, when the DMA content is sufficiently high, roughly above 50 mol%, PAND exhibits an opposite thermosensitivity, *i.e.*, LCST behavior, in aqueous solution. As shown in Fig. 3a, the aqueous solution of PAND<sub>52.6%</sub> at room temperature maintains a high transparency at both pH 3.5 and pH 2.0. Upon heating the pH 2 solution to 50 °C, the solubility of PAND<sub>52.6%</sub> is drastically decreased and the solution turns turbid. Like PAN, the LCST of PAND as measured with the cloud point, is also pH-sensitive. Fig. 3b shows the pH-dependent thermoresponsiveness of PAND<sub>52.6%</sub> aqueous solutions. When HCl is added to the solutions of PAND<sub>52.6%</sub>, a temperature-dependent solubility on-off switching appears, and their cloud point is gradually decreased. It can be seen in Fig. S11b† that the cloud point of PAND<sub>52.6%</sub> decreases from 59.5 to 33.1 °C when the pH decreases from 3.0 to 1.4. The LCST behavior of PAND appears similar to the effect of a hydrophobic

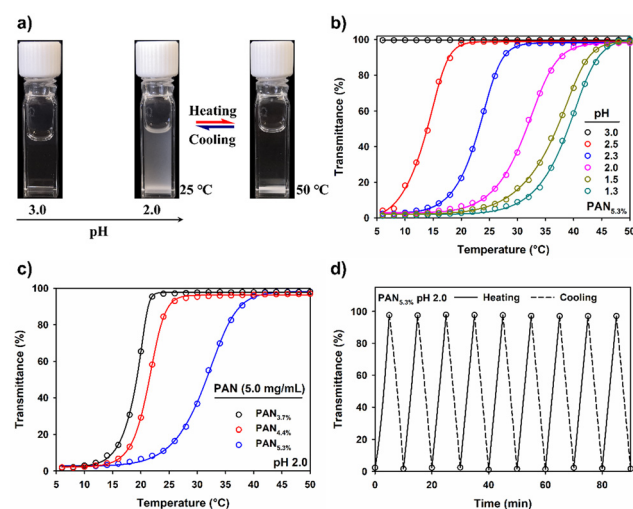


**Fig. 2** (a) Photographs of PAN<sub>5.3%</sub> solutions at room temperature with pH 3.0 and pH 2.0, and the solution with pH 2.0 at 50 °C, showing the UCST-type solubility. (b) Plots of solution transmittance (measured at 621 nm) vs. temperature for the aqueous solution of PAN<sub>5.3%</sub> (5.0 mg mL<sup>-1</sup>; heating rate: 1.0 °C min<sup>-1</sup>) at different pH values. (c) Plots of solution transmittance vs. temperature for PAN with different compositions in an aqueous solution at pH 2.0 (5.0 mg mL<sup>-1</sup>; heating rate: 1.0 °C min<sup>-1</sup>). (d) The reversible change of the transmittance of the aqueous solution of PAN<sub>5.3%</sub> (5.0 mg mL<sup>-1</sup>, pH 2.0) under nine consecutive heating (50 °C) and cooling (25 °C) cycles.

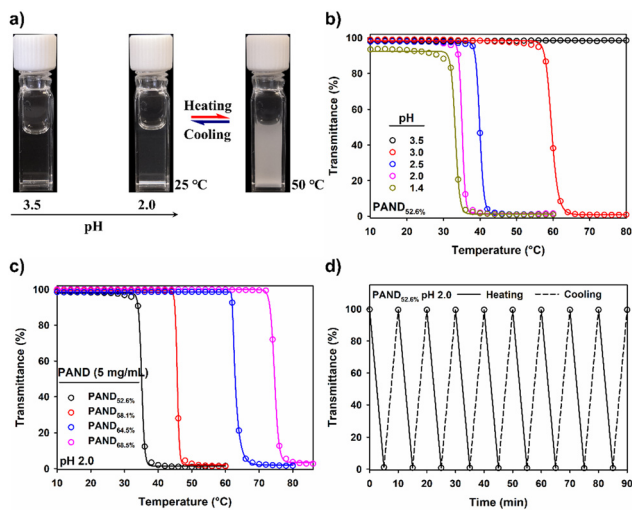


**Fig. 3** (a) Photographs of PAND<sub>52.6%</sub> solutions at room temperature with pH 3.5 and pH 2.0, and the solution with pH 2.0 at 50 °C. (b) Plots of solution transmittance vs. temperature for the aqueous solution of PAND<sub>52.6%</sub> (5.0 mg mL<sup>-1</sup>; heating rate: 1.0 °C min<sup>-1</sup>) at different pH values. (c) Plots of solution transmittance vs. temperature for PAND with different compositions in aqueous solution at pH 2.0 (5.0 mg mL<sup>-1</sup>; heating rate: 1.0 °C min<sup>-1</sup>). (d) The reversible change of the transmittance of the aqueous solution of PAND<sub>52.6%</sub> (5.0 mg mL<sup>-1</sup>, pH 2.0) under nine consecutive heating (50 °C) and cooling (25 °C) cycles.

comonomer on the LCST of PDMA,<sup>31</sup> but with the difference that in PAND, the H-bonded AA–NVCL and AA–AA play the role of a hydrophobic comonomer. Since, like in PAN, these H-bonds can be enhanced by the protonated COOH groups, the LCST transition can be reduced to lower temperature by lowering the pH of the copolymer solution. The LCST-type behavior of PAND has almost overlapping curves of transmittance vs. temperature and maintains a sharp transition upon copolymer dilution from 5.0 to 1.0 mg mL<sup>-1</sup> (Fig. S12a†). To study the effect of copolymer composition (AA/NVCL/DMA ratio) on the cloud point, a series of copolymers with the same AA/NVCL molar ratio (9/1) but varying DMA content in the feed were synthesized (Table 1) and investigated. The results in Fig. 3c show that the cloud point is dependent on the copolymer composition and can span over a wide temperature range (35–75 °C). The presence of more hydrophobic AA–NVCL complexes and the decrease of the content of DMA both have an effect of decreasing the cloud point. The reversible LCST solubility switch can be seen in Fig. 3d, showing the transmittance change in the aqueous solution of PAND<sub>52.6%</sub> (5 mg mL<sup>-1</sup>, pH 2.0) under nine consecutive heating (50 °C) and cooling (25 °C) cycles.

### Elucidation of opposite thermoresponsive solubility

In aqueous solution at a similar range of pH, PAN<sub>5.3%</sub> and PAND<sub>52.6%</sub> exhibit exactly opposite thermosensitivity, characterized by the UCST and LCST, respectively (Fig. 2 vs. Fig. 3). Nonetheless, they both show a similar pH-dependent cloud point, with increasing UCST and decreasing LCST upon

decreasing the pH. This result implies that H-bonding in both copolymers play the same determining role; *i.e.*, decrease in the pH enhances the formation of H-bonds between the comonomer units, especially in the strong H-bonded AA–NVCL complex generating the hydrophobic domain. In order to obtain more insight into these thermoresponsive behaviors, further characterization was performed. On the one hand, temperature-dependent DLS measurements were carried out to monitor the change in the size of copolymer aggregates under temperature or pH variations. Firstly, the results indicated the presence of only unimers in the solution of PAN<sub>5.3%</sub> at pH 3.0 and in the solution of PAND<sub>52.6%</sub> at pH 3.5 (hydrodynamic diameter  $D_H$  about 2 nm, Fig. S13a and S13c†); at these pH values, both samples are completely soluble over the temperature range investigated. Then, when the pH is decreased at room temperature, while PAN<sub>5.3%</sub> become insoluble forming large aggregates (Fig. S13b†), PAND<sub>52.6%</sub> forms only small aggregates with  $D_{TEM}$  around 10 nm (Fig. S15†) and the solution remains transparent. In Fig. 4a and c the DLS results of the two solutions under the same conditions are compared as in Fig. 2 and 3, *i.e.*, at pH 2.0 and upon changing the temperature from 25 to 50 °C, which further reveals the difference between the soluble state of PAN<sub>5.3%</sub> (50 °C) and PAND<sub>52.6%</sub> (25 °C): PAN chains are molecularly dissolved ( $D_H$  around 2 nm) prior to chain aggregation on cooling; in contrast, PAND are dispersed in the form of small micellar aggregates ( $D_H$  around 10 nm) before their aggregation on heating. These DLS results are consistent with the opposite UCST and LCST thermoresponsiveness of these two copolymers observed in the solution transmittance measurements. On the other hand, variable-temperature <sup>1</sup>H NMR spectra were recorded to confirm the hydration–dehydration transition of the copolymers in aqueous solution. In Fig. 4b, the characteristic resonance peaks of NVCL in the PAN copolymer from 3.1 to

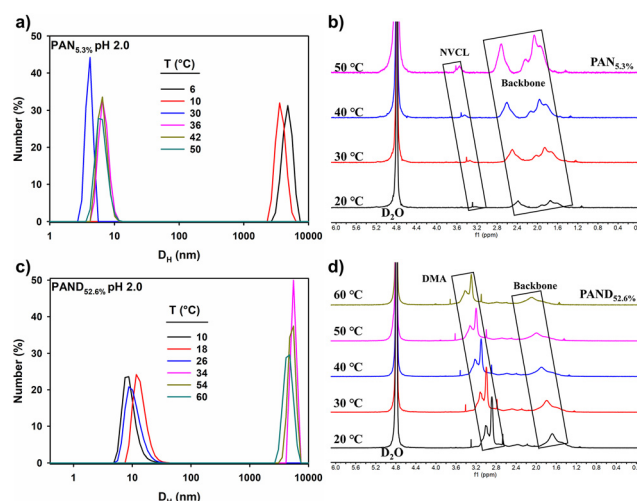


**Fig. 4** DLS-determined size distribution of the copolymer solutions at different temperatures at pH 2.0: (a) PAN<sub>5.3%</sub> and (c) PAND<sub>52.6%</sub> (5.0 mg mL<sup>-1</sup>). Variable-temperature <sup>1</sup>H NMR spectra of (b) PAN<sub>5.3%</sub> and (d) PAND<sub>52.6%</sub> in D<sub>2</sub>O (2.0 mg mL<sup>-1</sup>, pH 2.0).

3.6 ppm become much more visible and their intensities are significantly increased during heating, indicating a more soluble state of the NVCL groups in the copolymer chains. In contrast to PAN, the characteristic resonance signals for the PAND copolymer are visible at 20 °C, while upon heating the solution to 60 °C, the peaks of DMA from 2.8 to 3.5 ppm are reduced due to the aggregation of the DMA groups in the PAND copolymer chains (Fig. 4d). The signal changes in the protons are attributed to the fact that the chain backbone at a lower ppm also corroborates with the UCST behavior of PAN and the LCST behavior of PAND.

The different thermosensitivities of PAN<sub>5.3%</sub> and PAND<sub>52.6%</sub> as revealed by the measurement results can be schematically recapitulated as shown in Fig. 5. PAN and PAND are molecularly dissolved in aqueous solution at 25 °C with pH 3 and pH 3.5, respectively, when there is no H-bond formation due to ionized carboxylic acid groups. As the solution pH is lowered to pH 2, PAN becomes insoluble with the formation of large aggregates ( $D_H > 1000$  nm) due to H-bonding in the protonated COOH (AA–NVCL and AA–AA) and the solution turns turbid. As for PAND, the solution remains transparent, but small micellar aggregates ( $D_H$  around 10 nm) are formed due to H-bonding (AA–NVCL, AA–AA and AA–DMA) that endows PAND with an amphiphilic character. At pH 2, when the solution temperature is increased to 50 °C, PAN becomes soluble as H-bonds formed between the comonomer units are weakened, which accounts for the UCST thermosensitivity. In contrast, upon heating to 50 °C, the solution of PAND becomes turbid as a result of the aggregation of small micelles. This LCST thermosensitivity is also governed by H-bonding, particularly the hydrophobic H-bonded AA–NVCL complex, which exerts the same effect as a hydrophobic comonomer on PDMA by decreasing its LCST to an observable temperature range (ref. DMA with styrene<sup>31</sup>). Basically, upon heating, soluble DMA segments undergo a hydration–dehydration transition, which results in the aggregation of small micelles and the apparent insolubility of the copolymer once the temperature increases above the LCST. The fact that the hydrogen bonds of AA–NVCL and AA–AA can be enhanced by protonated COOH groups indi-

cates that they are sensitive to the pH change of the solution, which, in turn, leads to pH-tunable UCST and LCST.

### UCST and LCST hydrogels for information encryption and decryption

Based on the pH-induced diverse thermoresponsive behaviors of water-soluble copolymers, the security paper-inspired polymer hydrogels<sup>45,46</sup> with information recording, encryption, and decryption were prepared using PAN and PAND (ESI†). On the one hand, we employed an acid ink-containing pen to write information on the surface of the polymer hydrogel. As shown in Fig. 6a, when the acid-containing pen (HCl, 2.0 mol L<sup>-1</sup>) is in contact with the PAN hydrogel surface at room temperature, an obvious change in the transparency occurs due to the phase separation in the UCST hydrogel. When immersed in a hot bath of 50 °C (the UCST for PAN hydrogels is roughly 40 °C, Fig. S16a†), the recorded information is deleted. On cooling to 25 °C, the hydrogel returns to its original appearance, bringing back the recorded information. With the LCST-type hydrogel of PAND, the same information recording can be achieved using the acid ink pen, but the thermal encryption and decryption process is reversed due to the opposite temperature dependent solubility of the hydrogel. As an example, we have inscribed the symbol “+” on the surface of the hydrogel at room temperature (Fig. 6b), the symbol is initially invisible but becomes visible after placing the hydrogel at 50 °C (the LCST for PAND hydrogels is roughly 35 °C, Fig. S16b†); while the symbol almost vanishes on cooling the hydrogel to room temperature. Such encryption and decryption of the

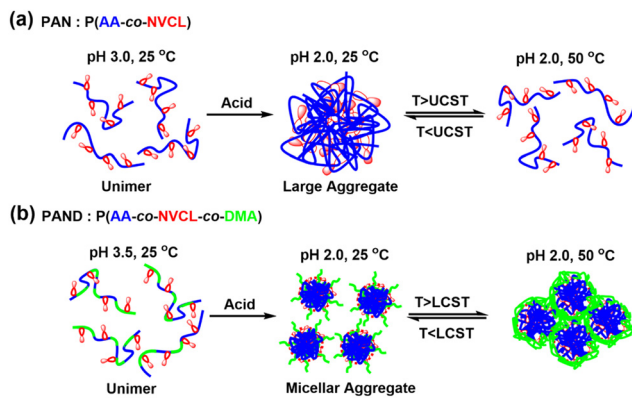


Fig. 5 Schematic illustration of the diverse thermoresponsive behaviors of (a) PAN and (b) PAND in aqueous solutions.

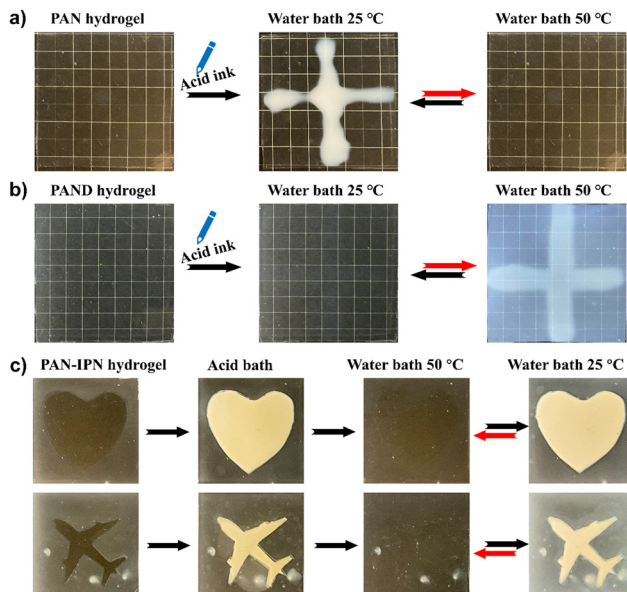


Fig. 6 Photographs showing different encryption and decryption processes upon heating (in a hot bath, 50 °C) and cooling (in a cold hot bath, 25 °C) of (a) PAN hydrogel, (b) PAND hydrogel, and (c) PAN-IPN hydrogel. In the case of PAN-IPN, the initial “latent” image is inscribed through the formation of a PAN/PAAm interpenetrating network in selected areas determined by a photomask (see the text for details).

acid-inscribed information was reversible under several heating and cooling cycles. It is worth mentioning that the acid-recorded information can be completely erased by immersing the hydrogels in an aqueous solution at higher pH to deprotonate the COOH groups. After the erasure process, the UCST or LCST hydrogel can be utilized again to record the new information with the acid ink pen.

As shown in Fig. 6c, other information inscription and encryption/decryption methods can be applied with the hydrogels. In this case, a piece of PAN hydrogel was first swollen in an aqueous solution (50 mL) of acrylamide (AAm, 1.0 mol L<sup>-1</sup>), I2959 (1.0 mg mL<sup>-1</sup>, photoinitiator) and MBA (3.0 mg mL<sup>-1</sup>, crosslinker), and then exposed to UV light through a photomask for photopolymerization in areas determined by the mask, resulting in a PAN/PAAm interpenetrating network (denoted as PAN-IPN) in those areas. Since the PAN-IPN loses the pH-sensitive UCST of PAN, a kind of “latent” image (corresponding to where no photopolymerization occurs) can be recorded in the hydrogel and subsequently developed in an acid bath (HCl, 2.0 mol L<sup>-1</sup>). Afterward, the reversible encryption and decryption can be processed by heating the hydrogel to 50 °C to make the “heart” and “airplane” images disappear, and cooling it to room temperature to bring the images back.

## Conclusions

We have synthesized random copolymers of PAN and PAND, which comprise two and three water-soluble monomers, respectively, and investigated their thermoresponsive behaviors in aqueous solution by means of solution transmittance, DLS and <sup>1</sup>H NMR measurements. While the UCST solubility change was found for PAN, LCST was observed for PAND (with PAN<sub>5.3%</sub> and PAND<sub>52.6%</sub> exhibiting exactly the opposite solubility switch between 25 and 50 °C at pH 2). In both cases, H-bonding between the comonomer units governs their thermoresponsive behavior, which provides the basis of a facile strategy for inducing the UCST or LCST in water-soluble polymers. Indeed, it was found that the thermoresponsiveness of PAN and PAND can be generated when the carboxylic acid groups are protonated by adjusting the pH of their aqueous solutions. The UCST behavior of PAN originates from H-bonded AA-NVCL and AA-AA which cause the insoluble state; as the H-bonding between the moieties in the polymer is weakened with the increase in temperature, the transition to the soluble state of PAN chains occurs on heating. As for the LCST behavior of PAND, H-bonded AA-NVCL and AA-AA exert a similar effect as a hydrophobic comonomer on the hydrophilic PDMA, which brings the hydration-dehydration transition on heating (LCST) of PDMA to an observable temperature range. Since the strength and the number of AA-NVCL and AA-AA H-bonds are both determined by the number of protonated COOH groups, both the UCST of PAN and the LCST of PAND are sensitive to the pH of the solution, as revealed by a pH-tunable cloud point (for a given copolymer composition and concentration). To demonstrate the potential

utility of the diverse thermoresponsive behaviors of these copolymers, we prepared their hydrogels and showed how information can be inscribed through pH-induced solubility switching of the hydrogel and how opposite encryption/decryption by varying the temperature can be achieved by making use of the UCST and LCST behaviors. These characteristics set them apart from conventional thermoresponsive hydrogels and impart them with the potential to develop a new class of thermoresponsive materials.

## Author contributions

The manuscript was written through contributions of all authors. All authors have given approval to the final version of the manuscript.

## Conflicts of interest

There are no conflicts to declare.

## Acknowledgements

Y. Zhao acknowledges the financial support from the Natural Sciences and Engineering Research Council of Canada (NSERC), le Fonds de recherche du Québec: nature et technologies (FRQNT), and The Centre Québécois sur les Matériaux Fonctionnels (CQMF). R. Cheng is grateful to the China Scholarship Council (CSC) for providing him with a scholarship to study and live in Canada. J. Jiang thanks the CSC for awarding her a scholarship. J. Hou thanks FRQNT for awarding him a scholarship.

## References

- 1 D. Roy, W. L. A. Brooks and B. S. Sumerlin, *Chem. Soc. Rev.*, 2013, **42**, 7214.
- 2 C. Z. Zhao, Z. Y. Ma and X. X. Zhu, *Polym. Sci.*, 2019, **90**, 269.
- 3 S. L. Qiao and H. Wang, *Nano Res.*, 2018, **11**, 5400.
- 4 Y. Hiruta, M. Shimamura, M. Matsuura, Y. Maekawa, T. Funatsu, Y. Suzuki, E. Ayano, T. Okano and H. Kanazawa, *ACS Macro Lett.*, 2014, **3**, 281.
- 5 Y. A. Wang, Y. Kotsuchibashi, Y. Liu and R. Narain, *Langmuir*, 2014, **30**, 2360.
- 6 J. Lee, K. H. Ku, M. Kim, J. M. Shin, J. Han, C. H. Park, G. R. Yi, S. G. Jang and B. J. Kim, *Adv. Mater.*, 2017, **29**, 1700608.
- 7 H. C. Tao, E. Galati and E. Kumacheva, *Macromolecules*, 2018, **51**, 6021.
- 8 H. Zhang, X. Tong and Y. Zhao, *Langmuir*, 2014, **30**, 11433.
- 9 C. Z. Zhao, J. L. Lu and X. X. Zhu, *ACS Appl. Polym. Mater.*, 2020, **2**, 256.
- 10 A. Abdollahi, H. Roghani-Mamaqani, B. Razavi and M. Salami-Kalajahi, *Polym. Chem.*, 2019, **10**, 5686.

11 Y. Stetsyshyn, K. Awsiuk, V. Kusnezh, J. Raczkowska, B. R. Jany, A. Kostruba, K. Harhay, H. Ohar, O. Lishchynskyi, Y. Shymborska, Y. Kryvenchuk, F. Krok and A. Budkowski, *Appl. Surf. Sci.*, 2019, **463**, 1124.

12 M. W. Tibbitt, J. E. Dahlman and R. Langer, *J. Am. Chem. Soc.*, 2016, **138**, 704.

13 X. Gu, J. J. Wang, X. F. Liu, D. P. Zhao, Y. N. Wang, H. Gao and G. L. Wu, *Soft Matter*, 2013, **9**, 7267.

14 D. Schmaljohann, *Adv. Drug Delivery Rev.*, 2006, **58**, 1655.

15 R. M. P. Da Silva, J. F. Mano and R. L. Reis, *Trends Biotechnol.*, 2007, **25**, 577.

16 K. Uhlig, T. Wegener, J. He, M. Zeiser, J. Bookhold, I. Dewald, N. Godino, M. Jaeger, T. Hellweg, A. Fery and C. Duschl, *Biomacromolecules*, 2016, **17**, 1110.

17 N. Yan, J. G. Zhang, Y. Yuan, G. T. Chen, P. J. Dyson, Z. C. Li and Y. Kou, *ChemComm*, 2010, **46**, 1631.

18 H. A. Zayas, A. Lu, D. Valade, F. Amir, Z. F. Jia, R. K. O'Reilly and M. J. Monteiro, *ACS Macro Lett.*, 2013, **2**, 327.

19 Y. H. Chen, Z. W. Wang, Y. W. Harn, S. Pan, Z. L. Li, S. L. Lin, J. Peng, G. Z. Zhang and Z. Q. Lin, *Angew. Chem., Int. Ed.*, 2019, **58**, 11910.

20 Y. H. Zheng, A. H. Soeriyadi, L. Rosa, S. H. Ng, U. Bach and J. J. Gooding, *Nat. Commun.*, 2015, **6**, 8797.

21 P. C. Zhao, M. J. Ni, C. Chen, Z. D. Zhou, X. P. Li, C. Y. Li, Y. X. Xie and J. J. Fei, *Nanoscale*, 2019, **11**, 7394.

22 S. Ryu, I. Yoo, S. Song, B. Yoon and J. M. Kim, *J. Am. Chem. Soc.*, 2009, **131**, 3800.

23 J. Li, Q. Y. Ma, Y. Xu, M. M. Yang, Q. Wu, F. F. Wang and P. C. Sun, *ACS Appl. Mater. Interfaces*, 2020, **12**, 55290.

24 Z. F. Sun, Y. Yamauchi, F. Araoka, Y. S. Kim, J. Bergueiro, Y. Ishida, Y. Ebina, T. Sasaki, T. Hikima and T. Aida, *Angew. Chem., Int. Ed.*, 2018, **57**, 15772.

25 Z. H. Zhang, Y. Wang, Q. Wang and L. R. Shang, *Small*, 2022, 2105116.

26 E. S. Gil and S. M. Hudson, *Prog. Polym. Sci.*, 2004, **29**, 1173.

27 F. D. Jochum and P. Theato, *Chem. Soc. Rev.*, 2013, **42**, 7468.

28 I. Dimitrov, B. Trzebicka, A. H. E. Muller, A. Dworak and C. B. Tsvetanov, *Prog. Polym. Sci.*, 2007, **32**, 1275.

29 Q. L. Zhang, C. Weber, U. S. Schubert and R. Hoogenboom, *Horizons*, 2017, **4**, 109.

30 H. Feil, Y. H. Bae, J. Feijen and S. W. Kim, *Macromolecules*, 1993, **26**, 2496.

31 M. Nichifor and X. X. Zhu, *Polymer*, 2003, **44**, 3053.

32 J. Niskanen and H. Tenhu, *Polym. Chem.*, 2017, **8**, 220.

33 J. Seuring and S. Agarwal, *ACS Macro Lett.*, 2013, **2**, 597.

34 J. Seuring and S. Agarwal, *Macromol. Rapid Commun.*, 2012, **33**, 1898.

35 L. D. Blackman, P. A. Gunatillake, P. Cass and K. E. S. Locock, *Chem. Soc. Rev.*, 2019, **48**, 757.

36 T. Maji, S. Banerjee, Y. Biswas and T. K. Mandal, *Biomacromolecules*, 2015, **48**, 4957.

37 L. Chen, Y. Honma, T. Mizutani, D. J. Liaw, J. P. Gong and Y. Osada, *Polymer*, 2000, **41**, 141.

38 H. Zhang, S. W. Guo, W. Z. Fan and Y. Zhao, *Macromolecules*, 2016, **49**, 1424.

39 A. Augé, F. Camerel, A. Benoist and Y. Zhao, *Polym. Chem.*, 2020, **11**, 3863.

40 C. Z. Zhao, L. Dolmans and X. X. Zhu, *Macromolecules*, 2019, **52**, 4441.

41 B. A. Pineda-Contreras, F. Y. Liu and S. Agarwal, *J. Polym. Sci., Part A: Polym. Chem.*, 2014, **52**, 1878.

42 N. An, X. H. Wang, Y. X. Li, L. Zhang, Z. Y. Lu and J. Q. Sun, *Adv. Mater.*, 2019, **31**, 1904882.

43 S. Ponratnam and S. L. Kapur, *J. Polym. Sci., Polym. Chem. Ed.*, 1976, **14**, 1987.

44 J. L. Lu, M. D. Xu, Y. Lei, L. H. Gong and C. Z. Zhao, *Macromol. Rapid Commun.*, 2021, **41**, 2000661.

45 C. T. Yu, K. P. Cui, H. L. Guo, Y. N. Ye, X. Y. Li and J. P. Gong, *Macromolecules*, 2021, **54**, 9927.

46 Z. Chen, Y. J. Chen, Y. T. Guo, Z. Yang, H. Li and H. Z. Liu, *Adv. Funct. Mater.*, 2022, 2201009.